



## DNP enhanced NMR with flip-back recovery

Snædís Björgvinsdóttir, Brennan J. Walder, Arthur C. Pinon, Jayasubba Reddy Yarava, Lyndon Emsley\*

Institut des Sciences et Ingénierie Chimiques, Ecole Polytechnique Fédérale de Lausanne (EPFL), CH-1015 Lausanne, Switzerland

### ARTICLE INFO

#### Article history:

Received 7 December 2017

Revised 24 January 2018

Accepted 27 January 2018

Available online 31 January 2018

#### Keywords:

Solid-state NMR

Dynamic nuclear polarization

Flip-back

Cross-polarization

Spin diffusion

### ABSTRACT

DNP methods can provide significant sensitivity enhancements in magic angle spinning solid-state NMR, but in systems with long polarization build up times long recycling periods are required to optimize sensitivity. We show how the sensitivity of such experiments can be improved by the classic flip-back method to recover bulk proton magnetization following continuous wave proton heteronuclear decoupling. Experiments were performed on formulations with characteristic build-up times spanning two orders of magnitude: a bulk BDPA radical doped *o*-terphenyl glass and microcrystalline samples of theophylline, L-histidine monohydrochloride monohydrate, and salicylic acid impregnated by incipient wetness. For these systems, addition of flip-back is simple, improves the sensitivity beyond that provided by modern heteronuclear decoupling methods such as SPINAL-64, and provides optimal sensitivity at shorter recycle delays. We show how to acquire DNP enhanced 2D refocused CP-INADEQUATE spectra with flip-back recovery, and demonstrate that the flip-back recovery method is particularly useful in rapid recycling regimes. We also report Overhauser effect DNP enhancements of over 70 at 592.6 GHz/900 MHz.

© 2018 The Author(s). Published by Elsevier Inc. This is an open access article under the CC BY-NC-ND license (<http://creativecommons.org/licenses/by-nc-nd/4.0/>).

### 1. Introduction

Cross-polarization magic angle spinning (CP MAS) NMR is the cornerstone experiment in solid-state NMR [1,2]. The sensitivity of conventional CP MAS experiments depends on the proton spin-lattice relaxation time, as it is the proton spin reservoir from which the rare nuclei draw their polarization. Many organic solids, however, have long proton spin-lattice relaxation times, which for rigid compounds can approach one hour. When combined with the low natural abundance and gyromagnetic ratio of important rare nuclei such as  $^{13}\text{C}$  and  $^{15}\text{N}$  this severely limits the sensitivity of CP MAS experiments. The acquisition of one-dimensional spectra with usable signal-to-noise ratios is particularly difficult in such cases, and multi-dimensional experiments are usually precluded.

In the early days of CP, resolution of the rare spin spectrum was improved by decoupling using spin locking of the proton magnetization during acquisition with a high power “continuous wave” (cw) rf field [1]. After acquisition, a significant fraction of the original proton magnetization remained, dephasing only upon release of the spin locking field. Since the very inception of cross-polarization, it was recognized that the residual proton magnetization could be further utilized to improve the signal-to-noise ratio of the rare spin spectrum, and to this end strategies such as multi-

ple contact/acquisition schemes were proposed [1]. The method of using a  $\pi/2$  pulse to return the residual proton magnetization to the z-axis after acquisition to allow a shorter recovery period was introduced by Tegenfeldt and Haerberlen in 1979 [3]. Owing to its facile implementation, use of this flip-back recovery method increased throughout the subsequent decades, with examples including work on zeolites [4], bacteriorhodopsin [5] and multidimensional  $^{13}\text{C}$  tensor correlation experiments on saccharides [6,7].

With the introduction of TPPM decoupling in 1995 [8], followed by other modern heteronuclear decoupling methods such as SPINAL-64 [9] it became more difficult to lock the proton magnetization during decoupling [10], and the flip-back experiment largely fell into disuse. However, the flip-back pulse element remains essential to schemes such as those used in quantitative cross-polarization methods [11], RELOAD-CP [12], dissolution DNP [13], and the suppression of water signals in solution NMR [14]. Recently, classic flip-back has been shown to be useful in the context of fast MAS, where efficient heteronuclear decoupling at sample rotation rates  $> 50$  kHz can be provided by low power cw spin locking fields [15,16].

Solid-state magic-angle-spinning dynamic nuclear polarization (DNP) can provide exquisite enhancements in overall sensitivity for a range of materials from frozen solutions to microcrystalline powders [17–20]. Most strategies involve the generation of hyperpolarization close to a radical source and transportation of this polarization to the target substrate by spontaneous proton spin dif-

\* Corresponding author.

E-mail address: [lyndon.emsley@epfl.ch](mailto:lyndon.emsley@epfl.ch) (L. Emsley).

fusion [21,22]. This is followed by conventional cross-polarization transfer of the enhanced proton polarization from the proton bath to the rare spins. For example, the use of incipient wetness impregnation DNP for microcrystalline systems can enhance the sensitivity of CP MAS experiments by factors of 100 or more at temperatures of 100 K [19]. However, since the polarization must be transported, the overall sensitivity of relayed DNP experiments is throttled by the long build up times needed to optimize sensitivity.

Here we show that flip-back methods can significantly improve the overall sensitivity of MAS DNP experiments.

## 2. Experimental

Salicylic acid, L-histidine monohydrochloride monohydrate and theophylline were obtained from Sigma Aldrich. The samples were ground by hand with a mortar and pestle for 5 min and subsequently wetted with a 16 mM solution of TEKPol [23] in 1,1,2,2-tetrachloroethane (TCE), [24] which dissolves the radical but is a non-solvent for the powders [18]. The formulation ratio was 10  $\mu$ L of radical solution to 40 mg of powdered solid. The wet powder was packed in a 3.2 mm sapphire rotor and centered with a polytetrafluoroethylene insert.

All experiments on microcrystalline samples were performed on a widebore 9.4 T Bruker Avance III solid-state NMR spectrometer coupled with a 263 GHz microwave source [25]. The samples were spun in a 3.2 mm low-temperature MAS probe at a rate of 12.5 kHz at temperatures near 90 K. To improve enhancements, the samples were deoxygenated with three thawing cycles by repeated ejection and insertion of the sample in the NMR probe [26]. Polarization enhancement factors of the TCE protons were estimated from comparing proton spectra at a 5 s recycle delay with and without microwave irradiation, indicating enhancements over 200 for L-histidine monohydrochloride monohydrate and salicylic acid. The enhancement of the theophylline system could not be estimated in this way because of substantial recovery of the theophylline protons due to their short intrinsic proton  $T_1$ . On the basis of CP spectra with and without microwave irradiation (Fig. S1), the TCE enhancement of the theophylline system is similar to that of the other two microcrystalline systems.

BDPA ( $\alpha,\gamma$ -bis(diphenylene- $\beta$ -phenylallyl)) was obtained from Sigma Aldrich and dissolved in partly deuterated ortho-terphenyl (95:5 OTP- $d_{14}$ :OTP). The resulting 75 mM solution was melted in a 3.2 mm rotor, topped with a polytetrafluoroethylene insert and rapidly inserted into a cold NMR probe.

Overhauser effect DNP experiments [27] on BDPA in OTP [28] were carried out at 21.14 T using a Bruker Avance Neo spectrometer. The frequency of the microwave beam could be lowered to reach the Overhauser effect condition from the optimum binitroxide cross effect condition by changing the temperature of the resonant cavity (Fig. S2). The OTP sample was spun at a rate of 12.5 kHz in a low-temperature MAS probe. The signal enhancement factor,  $\epsilon_c$ , as indicated by the ratio of signal with and without microwave irradiation was 73 (Fig. S3).

Unless otherwise specified, a 93 kHz radio-frequency field amplitude was used for the heteronuclear decoupling fields. For XiX decoupling [29] the pulse widths used were 640  $\mu$ s. CP contact time was 2 ms for the microcrystalline solids and 4 ms for the OTP glass. The  $^1\text{H}$  rf field amplitude was ramped from 90% to 100% during CP for all compounds. The acquisition time for the microcrystals was 26 ms and 4 ms for the OTP system. In order to reach a steady state condition, a number of dummy scans, roughly equal to 10% of the scans used during data accumulation, were implemented for the flip-back experiments. The experiments were performed in order of high to low values of recycle delay, further

minimizing the change in steady state condition between consecutive experiments.

For the INADEQUATE experiments, 20 complex  $t_1$  points at an indirect sampling interval of  $\Delta t_1 = 0.16$  ms were acquired at effective 512 scans each for a total experiment time of  $\sim 14$  h. A 150 kHz radio-frequency field amplitude was used for decoupling.

We simulate the diffusion of polarization from the impregnating solution to the microcrystal using numerical simulations as described in detail elsewhere [22]. The resulting polarization is integrated over the microcrystal volume. The polarization is then scaled by the retention factor and propagated again during the subsequent polarization period. This procedure is repeated for the number of experimental scans. The resulting accumulated signal is then scaled by the number of loops, and by the square root of time, to obtain a sensitivity curve as a function of the recycle delay. This procedure is repeated for all recycle delays, numbers of scans, and the only variable parameter between the “with flip-back” case and “without flip-back” case is the retention factor.

## 3. Results and discussion

The fundamentals of bulk proton magnetization recovery using a flip-back pulse, as shown in Fig. 1a, and an excellent overview of the benefits of the sequence were given in the seminal work of Tegenfeldt and Haeberlen [3]. In a thermodynamic framework, the heat capacity of the abundant  $^1\text{H}$  spin reservoir far exceeds that of the rare  $^{13}\text{C}$  spin reservoir, particularly when the latter is present at natural abundance. As CP MAS NMR is usually practiced today, the proton magnetization is destroyed during acquisition by heteronuclear decoupling methods such as TPPM or SPINAL. Consequently, the magnetization must recover over a recycle delay  $\tau_{rd}$  prior to the execution of the following scan. In a simple exponential model of recovery from zero intensity, the degree to which the magnetization is restored during  $\tau_{rd}$  is given by

$$M_z(\tau_{rd}) = M_\infty \left[ 1 - \exp\left(-\frac{\tau_{rd}}{T_B}\right) \right]. \quad (1)$$

We introduce the build-up time constant,  $T_B$ , in this expression to acknowledge that in DNP the magnetization does not usually recover according to the intrinsic spin-lattice relaxation time,  $T_1$ , of the substrate [30]. Only for conventional NMR of a pure solid analyzed in the absence of the exogenous source of polarization is  $T_B = T_1$ . This is important, since in many DNP experiments  $T_B < T_1$ , and this is already a source of increased overall sensitivity for DNP enhanced solid-state NMR experiments [31–33].

At temperatures around 100 K or below, where MAS DNP experiments are today most efficient, there is often a more or less pronounced loss in spectral resolution due to freezing out molecular motions [34,35]. The cw method of heteronuclear decoupling can thus often be used with only a modest loss of resolution (*vide infra*). In this case, proton magnetization can be locked during decoupling and is depleted primarily through  $T_{1\rho}$  relaxation (and, to a lesser extent, direct polarization transfer to  $^{13}\text{C}$  nuclei). Upon flip-back, the longitudinal component of the proton magnetization,  $M_z$ , resumes its build up toward  $M_\infty$ , but at a significant nonzero initial amplitude. Under steady state conditions, this implies that

$$M_z(0) = f_0 M_z(\tau_{rd}). \quad (2)$$

where  $f_0$ , the retention factor, is the ratio of bulk proton magnetization before and after the CP experiment.  $f_0$  is an empirical parameter that depends on many factors in the experiment, including notably  $T_{1\rho}$ , the efficiency of the pulses, off resonance effects, and the decoupling sequence used. For decoupling methods such as TPPM,  $f_0$  is usually zero, and the initial level of magnetization available for subsequent scans is also zero.

Assuming that the dynamics of CP transfer is independent of  $f_0$  and  $\tau_{rd}$ , the intensity of the  $^{13}\text{C}$  NMR signals will be proportional to  $M_z$ . For a fixed experiment time, not only will the steady state value of  $M_z$  vary as a function of  $\tau_{rd}$ , but the number of scans and hence the signal that is accumulated will be inversely proportional to  $\tau_{rd}$ . The noise level of the final accumulated spectrum is inversely proportional to the square root of  $\tau_{rd}$ . Thus, in consideration of these effects, we arrive at the following equation for expressing the experimental sensitivity for a monoexponential model of magnetization recovery:

$$S_{rel}(f_0, \tau_{rd}) = \frac{A}{\sqrt{\tau_{rd}}} \frac{1 - \exp\left(-\frac{\tau_{rd}}{T_B}\right)}{1 - f_0 \exp\left(-\frac{\tau_{rd}}{T_B}\right)}, \quad (3)$$

where  $A$  is a normalization factor such that  $S_{rel}(0, \tau_{rd}^{(0)}) = 1$  with  $\tau_{rd}^{(0)} \approx 1.256T_B$ , which is the recycle delay where  $S_{rel}$  is maximized for the case  $f_0 = 0$ . This corresponds to the case of optimal sensitivity without flip-back. This function is plotted in Fig. 1b as a function of recycle delay for selected values of  $f_0$ . For the case  $f_0 = 0$ , we see that  $S_{rel} \leq 1$  for all values of  $\tau_{rd}$ , as guaranteed by our choice of normalization. When  $f_0 > 0$  sensitivity will be improved for all values of  $\tau_{rd}$ . The degree of improvement, however, is modest until  $f_0$  approaches unity, as illustrated by the fact that obtaining an 80% improvement in sensitivity over the reference experiment requires  $f_0 = 0.8$ , whereas a further improvement to almost 160% over the reference only requires an additional 12.5% increase in  $f_0$  to 0.9. Retaining half the magnetization ( $f_0 = 0.5$ ) only leads to a maximum improvement

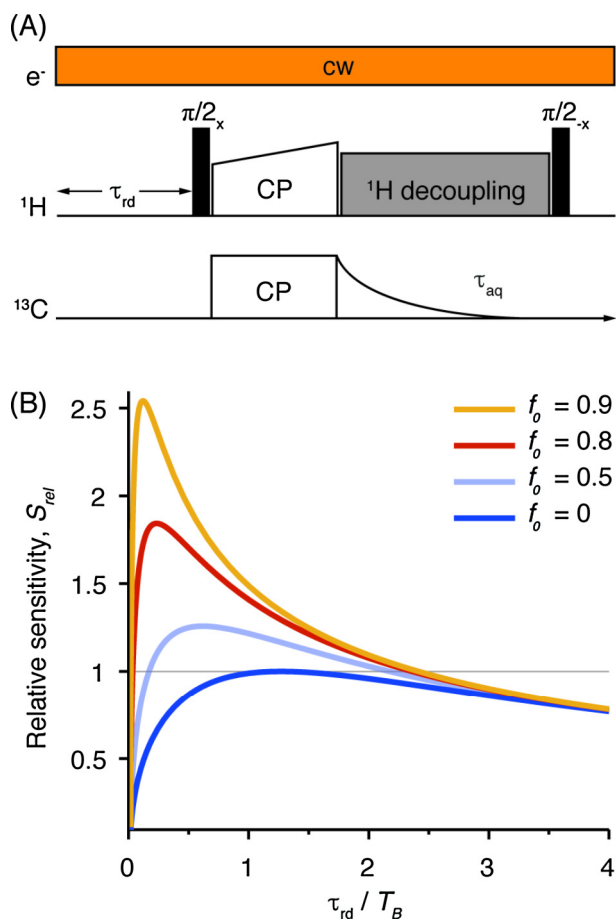


**Fig. 1.** (A) The  $^1\text{H}$ - $^{13}\text{C}$  CP pulse sequence with flip-back recovery. (B) Calculated gain in sensitivity for different values of  $f_0$  according to Eq. (3). The y-axis is normalized as defined in the text.

of 25%. High  $f_0$  values are thus the key to obtaining high sensitivity increase with flip-back.

In addition to the improvement in sensitivity, another advantage of proton magnetization recovery is that the recycle delay required to optimize the experimental sensitivity,  $\tau_{rd}^*$ , decreases with increasing  $f_0$ . We see from Fig. 1b that when 90% of proton magnetization can be recovered,  $\tau_{rd}^* \approx 0.1T_B$ , yielding an order of magnitude reduction in optimum recycle time compared to  $\tau_{rd}^{(0)}$  for the reference case.

To validate these features, we show results from CP MAS experiments of a frozen solution of BDPA in an OTP glass, enhanced by Overhauser effect (OE) DNP [27,28] at 21.14 T (the highest field used in DNP to date). The  $^1\text{H}$  DNP enhancement in this sample is  $\varepsilon = 73$ . Fig. 2 shows the sensitivity gains obtained experimentally using cw decoupling and flip-back. The major features predicted theoretically from the simple model of single exponential recovery are all illustrated by the experimental data. The sensitivity is never impaired when the flip-back pulse is included, no matter the recycle delay. The sensitivity maximum is found to occur at  $\tau_{rd}^* \approx 0.6\tau_{rd}^{(0)}$  and the maximum sensitivity enhancement due to the recovery is roughly 25%, corresponding to an  $f_0$  value of around 50%. Since the BDPA radical and OTP form a homogenous phase,  $T_{1\rho}$  processes are enhanced by paramagnetic relaxation [36], limiting the overall advantage due to the flip-back recovery. This could in principle be overcome by lowering the concentration of BDPA.

Microcrystalline solids polarized by relay should not suffer from relaxation enhancement by the paramagnetic agent. We therefore investigated three microcrystalline solids enhanced by relayed DNP: [19,22] theophylline, L-histidine monohydrochloride monohydrate, and salicylic acid. The compounds exhibit characteristic build-up time constants ranging over two orders of magnitude from 15 s for theophylline to over 1000 s for salicylic acid. (Note that form II of theophylline used here does not convert under impregnation with TCE) [37]. The measured values from a stretched exponential fit are given in the SI with the corresponding build up curves (Fig. S4).

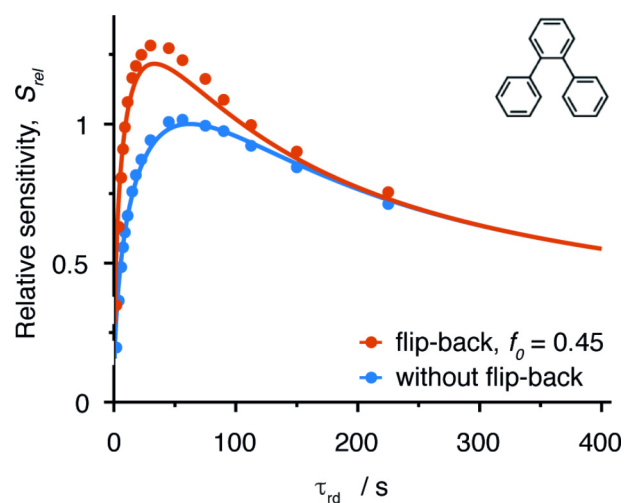


**Fig. 2.** Measured sensitivity gains (filled circles) using DNP enhanced flip-back CP MAS on a sample of 95:5 OTP- $d_{14}$ :OTP doped with 75 mM BDPA. Signal intensities from cw decoupled flip-back CP experiments (red dots) are compared to the same experiments without a flip-back pulse (blue dots). The rf field amplitude for decoupling was 100 kHz. The sensitivity is normalized to maximum sensitivity without a flip-back pulse. The curves are fit to the data with a monoexponential recovery model, as explained in the text. Raw data are provided in SI. (For interpretation of the references to colour in this figure legend, the reader is referred to the web version of this article.)

The maximum achievable sensitivity is roughly doubled for the theophylline and L-histidine monohydrochloride monohydrate samples, and nearly tripled for salicylic acid.

Spin diffusion models have previously shown that the build-up time in impregnated samples depends on several parameters such as the size of the microcrystals, the intrinsic longitudinal relaxation time, or the spin diffusion coefficient. Here the retention of proton magnetization,  $f_o$ , depends on position since  $T_{1\rho}$  is expected to be different in the impregnating radical solution and in the microcrystal. We have simulated the relayed DNP here with the retention of proton magnetization in the radical solution  $f_{o,RS}$  assumed to be 0.5 for all the simulations, and the signal build-up time  $T_{B,RS}$  was taken to be 2 s. The enhancement on the radical solution  $\epsilon_{RS}$  was assumed to be 280 for each case. We assume the spin diffusion constant in the radical solution to be  $D_{RS} = 1.7 \times 10^{-4} \mu\text{m}^2 \text{s}^{-1}$ . The spin diffusion constant within the microcrystals,  $D_{MC}$ , is scaled according to the proton concentration, as shown in Table 1. Note that  $f_{o,MC}$ , the retention factor within the substrate, will have an influence on the build-up time of the signal from the microcrystals, and thus on the sensitivity.

The data are well reproduced with the parameters given in Table 1, which lead to the curves shown in the figures, where  $L$  corresponds to the diameter of the spherical particles,  $D_{MC}$  is the diffusion rate inside the particle, and  $T_{1,MC}$  is the intrinsic longitudinal relaxation time. Note that fits to exponential and stretched exponential recovery models, failed to reproduce the data, as shown in Fig. S5.

We note that these simulations suggest retention factors between 0.6 and 0.9 can be achieved with cw decoupling under DNP conditions. These retention factors are reasonable given that our estimated  $T_{1\rho,MC}(^1\text{H}) > 100$  ms for the microcrystalline solids exceeds the  $^{13}\text{C}$  acquisition time of 26 ms. If we consider from Fig. 1 that relative sensitivity grows most rapidly between 0.9 and 1.0, this indicates that if the recovery factors could be increased further still by, for example, increasing the strength of the cw spin lock during signal acquisition on the  $^{13}\text{C}$  channel, then the experiment may become even more efficient.

Increasing the cw decoupling power also leads to line narrowing in  $^{13}\text{C}$  spectra by increasing the coherence lifetime during signal acquisition,  $T_2^*$ . Of course, the improvement in resolution is concomitant to an improvement of the signal-to-noise ratio and hence sensitivity. Since continuous wave decoupling has fallen out of favor in the era of modern CP MAS NMR because of the lack of resolution provided by the method at practical rf field amplitudes, it is prudent to consider the effects of other decoupling methods on the sensitivity of flip-back experiments. Fig. 4 shows the  $^{13}\text{C}$  resonance of three of the carbons in the CP spectrum of L-histidine monohydrochloride monohydrate. In addition to cw, we consider decoupling by the XiX and SPINAL-64 schemes, and we give line widths measured at half height. This highlights an unsurprising general feature of the comparison; namely, that cw decoupling gives the poorest resolution and SPINAL-64 the best, with XiX in between.

The XiX decoupling method preserves a well-defined spin locking axis and is, in principle, amenable to proton magnetization recovery. We therefore consider the use of flip-back recovery with

**Table 1**  
Parameters used to reproduce the polarization dynamics shown in Figs. 3 and 5.

	$L/\mu\text{m}$	$D_{MC}/\mu\text{m}^2 \text{s}^{-1}$	$T_{1,MC}/\text{s}$	$f_{o,MC}$
Theophylline	2.4	$4.5 \cdot 10^{-4}$	10	0.77
Histidine (cw)	1.4	$5.1 \cdot 10^{-4}$	1000	0.65
Histidine (XiX)	1.4	$5.1 \cdot 10^{-4}$	1000	0.20
Salicylic acid	3.8	$4.3 \cdot 10^{-4}$	80,000	0.89

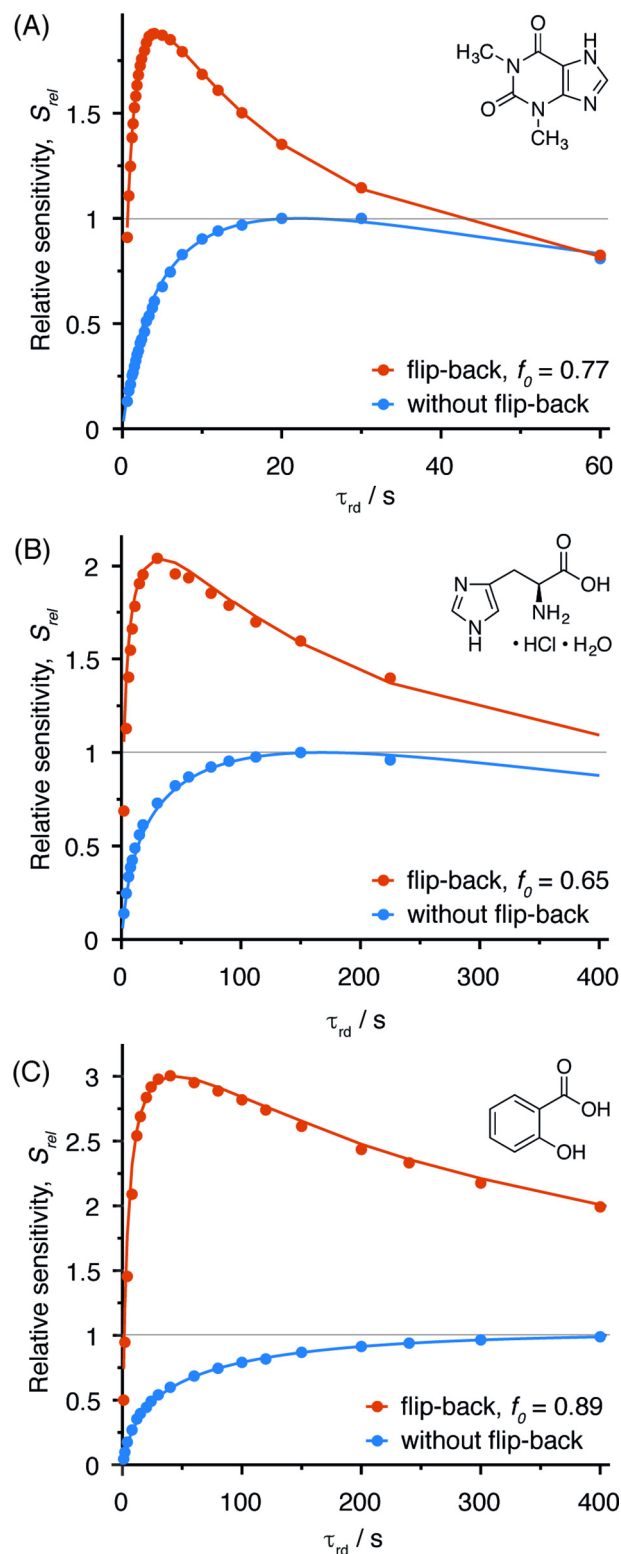


**Fig. 3.** Measured sensitivity gains (filled circles) using DNP enhanced flip-back CP MAS on samples of (A) theophylline, (B) L-histidine monohydrochloride monohydrate, and (C) salicylic acid, (using a carbonyl  $^{13}\text{C}$  resonance in each spectrum). Data for decoupled CP MAS without flip-back recovery (blue) was acquired for each sample as a sensitivity benchmark. The number of scans were adjusted to preserve a constant total acquisition time between experiments. Dummy scans were used for the flip-back experiment in order to achieve a steady-state polarization prior to each experiment. The solid lines are predictions from numerical simulations for  $f_o$  in the microcrystals according to a diffusion model of polarization transport. [22] Raw data are provided in SI. (For interpretation of the references to colour in this figure legend, the reader is referred to the web version of this article.)

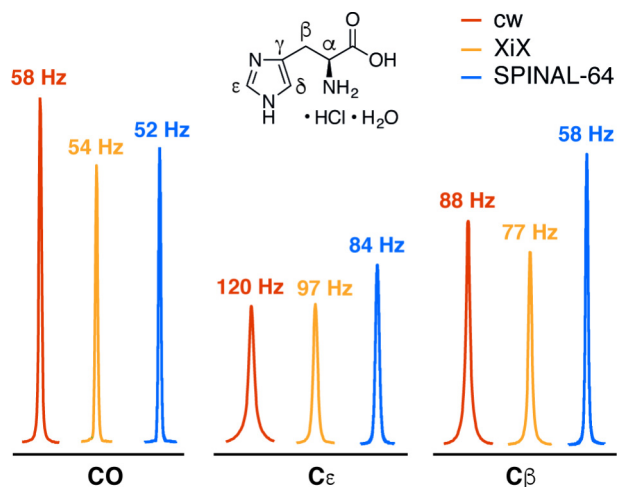


**Fig. 4.** Selected peaks from DNP enhanced  $^{13}\text{C}$  CP MAS spectra of L-histidine at a recycle delay of 150 s with 6 scans each. The spectra acquired with cw (with flip-back) and SPINAL-64 decoupling are respectively offset to the left and right of XiX decoupling (without flip-back) to facilitate comparison of the relative sensitivity of each  $^{13}\text{C}$  resonance. Line widths displayed are measured at half peak height.

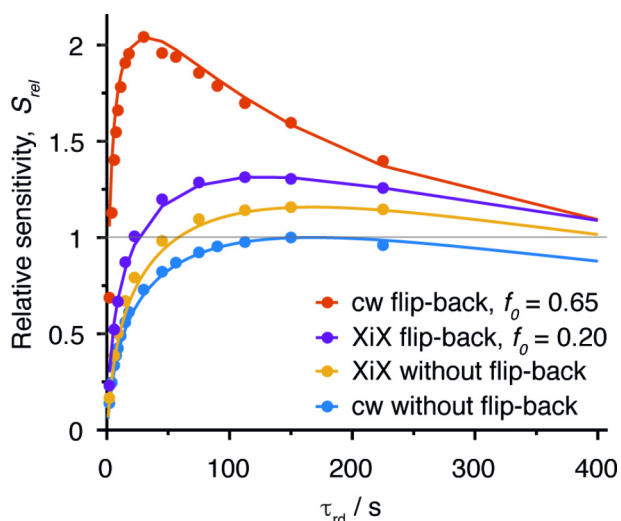


**Fig. 5.** Relative sensitivity of DNP enhanced flip-back CP MAS experiments for cw and XiX decoupling as a function of recycle delay for the  $^{13}\text{C}$  carbonyl resonance of L-histidine monohydrochloride monohydrate. Data for decoupled CP MAS without flip-back recovery (blue) was acquired as a sensitivity benchmark. In all cases the number of scans were adjusted to preserve a constant total acquisition time between experiments. Dummy scans were used to achieve a steady-state polarization prior to each experiment. (For interpretation of the references to colour in this figure legend, the reader is referred to the web version of this article.)

the XiX decoupling scheme. This comparison is given in Fig. 5 for  $^{13}\text{C}$  L-histidine monohydrochloride monohydrate.

We see by this comparison a modest sensitivity improvement of about 10% is possible by using XiX decoupling instead of cw. Most of the sensitivity advantage of the XiX method comes from the narrower linewidth. The figure also shows the result from flip back with XiX, where there is an improvement with respect to ordinary XiX acquisition, but it is relatively low since the  $f_0$  for this experiment is estimated to be around 0.2. This highlights that preservation of magnetization under more complex decoupling than cw is difficult. By far the best sensitivity is obtained with the cw flip-back experiment which here yields a factor 2 improvement. The price to pay in terms of resolution is relatively modest, going from 77 to 88 Hz for the  $\text{C}_\beta$  resonance as shown in Fig. 4.

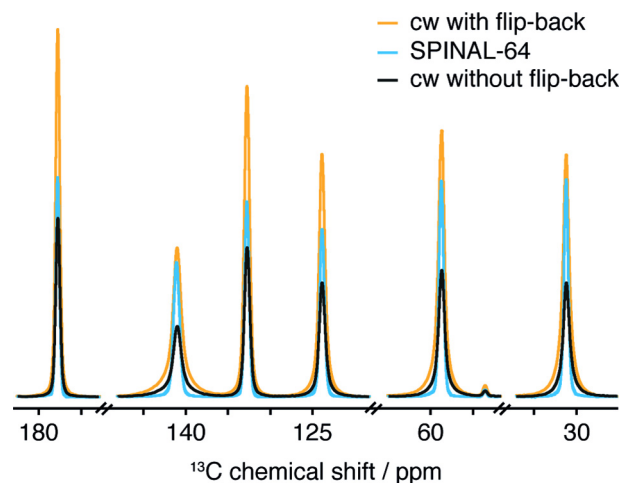


**Fig. 6.** Sensitivity optimized DNP enhanced  $^{13}\text{C}$  CP MAS spectra of L-histidine. A recycle delay of 150 s was used for the cw spectrum without flip-back and the spectrum implementing SPINAL-64 decoupling. A recycle delay of 30 s was used for the spectrum with a flip-back pulse. The number of scans were adjusted so the total experiment time was 15 min and each spectrum is displayed at the same level of noise. Consequently, the intensities correspond to the relative sensitivity of each  $^{13}\text{C}$  resonance.

In Fig. 6, three different sensitivity optimized  $^{13}\text{C}$  CP MAS spectra of L-histidine monohydrochloride monohydrate are compared. The superior line narrowing capability of SPINAL-64 at the rf field amplitudes used here improves the sensitivity from between 20% and 100%, depending on the signal of interest. In particular, the sensitivity of the carbonyl signal, which experiences weaker proton couplings than the carbons with directly attached protons, is improved only marginally by the switch to SPINAL-64. In spite of this, the sensitivity of the flip-back experiment with cw exceeds that of SPINAL-64 for each one of the carbon signals, despite the slightly inferior resolution. Here again, the advantage is most striking for the carbonyl signal. All resonances are well resolved in all cases.

For relayed DNP systems, it is known that solids with intrinsically high proton  $T_1$  values lead to higher polarization in the crystallites [22]. Further, in relayed DNP with long  $T_1$ , build-up times are limited by  $D$ , not  $T_1$ . The flip-back method compounds further advantages onto such systems by substantially and universally reducing the recycle delay required to reach a given level of sensitivity.

To demonstrate the power of the combined approach, Fig. 7 shows the application of the 2D refocused scalar CP-INADEQUATE experiment [38] to the impregnated salicylic acid sample. When DNP enhancements are high ( $\geq 100$ ) and polarization relay is efficient, INADEQUATE and similar  $^{13}\text{C}$ - $^{13}\text{C}$  correlation experiments on such samples become practical, but still generally require long periods of signal averaging [19]. In Fig. 7 the flip-back INADEQUATE spectrum shows all the expected through-bond correlations, and the  $^{13}\text{C}$  spectrum can be confidently assigned as shown. We observe that the quaternary carbon signals exhibit the greatest intensity. This is primarily attributed to more effective decoupling of these  $^{13}\text{C}$  nuclei by the cw field, such that they possess longer coherence lifetimes  $T_2'$  than  $^{13}\text{C}$  nuclei with attached protons and experience less dephasing during the mixing period [38]. To this result we compare the spectrum obtained with SPINAL-64 decoupling and no flip-back recovery. The sensitivity is significantly worse (as expected from the analysis on the previous figures), and only the two quaternary correlations are observed.

As Figs. 2 and 3 indicate, the sensitivity advantage of the flip-back recovery over the conventional cw experiment in the rapid

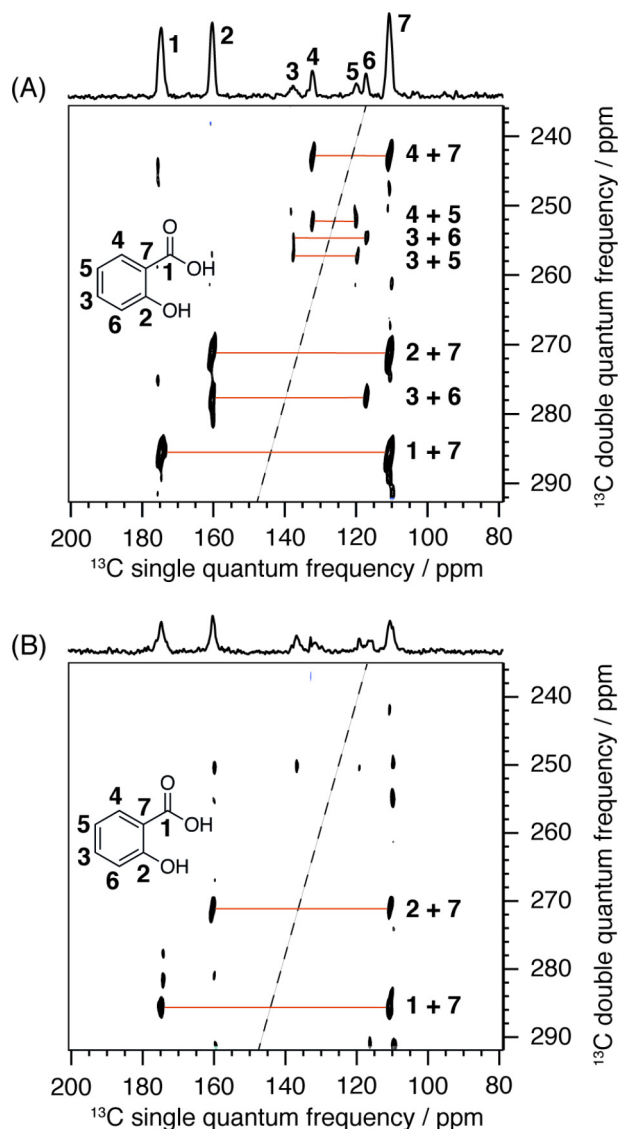


**Fig. 7.** (A) Two-dimensional DNP enhanced  $\{^{13}\text{C}\}$   $^{13}\text{C}$  refocused CP-INADEQUATE correlation spectrum of salicylic acid with cw proton decoupling and flip-back recovery of magnetization. All through-bond correlations are observed. (B) Comparable refocused CP-INADEQUATE spectrum without flip-back recovery using SPINAL-64 decoupling. Only two correlations are observed. The decoupling field amplitudes were  $\nu_1(^1\text{H}) = 150$  kHz. 64 dummy scans were used for the experiment implementing cw decoupling with flipback; presaturation was used instead for the SPINAL-64 implementation.

recycling regime  $\tau_{\text{rd}} \ll \tau_{\text{rd}}^* \approx 1$  min (assuming  $f_0 \approx 0.9$ ), where  $\tau_{\text{rd}}^*$  is the optimum recycle delay, can approach a factor of ten. This more than compensates the improvements in  $T_2^*$  and  $T_2'$  granted by SPINAL-64 decoupling and is the primary reason for the superior performance of the flip-back INADEQUATE experiment in our case.

Note that in cases where large numbers of scans are required, for example with long phase cycles, and where sensitivity is not limiting, the number of scans becomes limiting for the total experimental time. In that case, with flip-back, more scans can be achieved per unit time since the optimal recycle delays are always shorter, thus reducing total experimental time.

#### 4. Conclusions

The sensitivity of cross-polarization experiments on solids enhanced by relayed DNP can be further improved by recovering bulk proton magnetization with a flip-back pulse after an experi-

ment using continuous wave decoupling during acquisition on  $^{13}\text{C}$ . Using flip-back recovery always improves the sensitivity of such experiments and shifts the recycle delay which provides optimum sensitivity toward lower values. For practical rf field amplitudes, it is feasible to recover over 90% of the proton magnetization, which can triple the sensitivity over the experiment without flip-back recovery for samples with long  $T_B$ , and reduces the optimum recycle delay by over a factor of ten. Use of the continuous wave decoupling diminishes the sensitivity of the CP experiment by up to a factor of two compared to a state-of-the-art heteronuclear decoupling method such as SPINAL-64. Even so, the sensitivity of a flip-back optimized continuous wave decoupled experiment can easily exceed that of an experiment using SPINAL-64. When required, the combination of XiX decoupling and flip-back is representative of a compromise where sensitivity and resolution are improved over continuous wave while some level of enhancement using a flip-back pulse is retained. Despite relatively unfavorable effects on  $^{13}\text{C}$  coherence lifetimes during the mixing period and acquisition, the sensitivity of a continuous wave decoupled flip-back 2D INADEQUATE experiment on an impregnated sample of salicylic acid acquired in a rapid recycling regime significantly exceeds that of one acquired with SPINAL-64.

#### Acknowledgments

This work was supported by European Research Council Advanced Grant No. 320860 and Swiss National Science Foundation Grant No. 200021\_160112.

#### Appendix A. Supplementary material

Supplementary data associated with this article can be found, in the online version, at <https://doi.org/10.1016/j.jmr.2018.01.017>.

#### References

- [1] A. Pines, M.G. Gibby, J.S. Waugh, Proton-enhanced NMR of dilute spins in solids, *J. Chem. Phys.* 59 (2) (1973) 569–590.
- [2] J. Schaefer, E.O. Stejskal, C-13 nuclear magnetic-resonance of polymers spinning at magic angle, *J. Am. Chem. Soc.* 98 (4) (1976) 1031–1032.
- [3] J. Tegenfeldt, U. Haeberlen, Cross polarization in solids with flip-back of I-spin magnetization, *J. Magn. Reson.* (1969) 36 (3) (1979) 453–457.
- [4] G. Boxhoorn, A.G.T.G. Kortbeek, G.R. Hays, N.C.M. Alma, A high-resolution solid-state  $^{29}\text{Si}$  n.m.r. study of ZSM--5 type zeolites, *Zeolites* 4 (1) (1984) 15–21.
- [5] G.S. Harbison, S.O. Smith, J.A. Pardo, J.M.L. Courtin, J. Lugtenburg, J. Herzfeld, R.A. Mathies, R.G. Griffin, Solid-state carbon-13 NMR detection of a perturbed 6-s-trans chromophore in bacteriorhodopsin, *Biochemistry* 24 (24) (1985) 6955–6962.
- [6] M.H. Sherwood, D.W. Alderman, D.M. Grant, Two-dimensional chemical-shift tensor correlation spectroscopy. Multiple-axis sample-reorientation mechanism, *J. Magn. Reson.* (1969) 84 (1989) 466–489.
- [7] C.D. Hughes, M.H. Sherwood, D.W. Alderman, D.M. Grant, Chemical-shift-chemical - shift correlation spectroscopy in powdered solids, *J. Magn. Reson., Ser. A* 102 (1) (1993) 58–72.
- [8] A.E. Bennett, C.M. Rienstra, M. Auger, K.V. Lakshmi, R.G. Griffin, Heteronuclear decoupling in rotating solids, *J. Chem. Phys.* 103 (16) (1995) 6951–6958.
- [9] B.M. Fung, A.K. Khitrin, K. Ermolaev, An improved broadband decoupling sequence for liquid crystals and solids, *J. Magn. Reson.* 142 (1) (2000) 97–101.
- [10] G. De Paepe, B. Elena, L. Emsley, Characterization of heteronuclear decoupling through proton spin dynamics in solid-state nuclear magnetic resonance spectroscopy, *J. Chem. Phys.* 121 (7) (2004) 3165–3180.
- [11] R.L. Johnson, K. Schmidt-Rohr, Quantitative solid-state  $^{13}\text{C}$  NMR with signal enhancement by multiple cross polarization, *J. Magn. Reson.* 239 (2014) 44–49.
- [12] J.J. Lopez, C. Kaiser, S. Asami, C. Glaubitz, Higher sensitivity through selective  $^{13}\text{C}$  excitation in solid-state NMR spectroscopy, *J. Am. Chem. Soc.* 131 (44) (2009) 15970–15971.
- [13] S. Jannin, A. Bornet, S. Colombo, G. Bodenhausen, Low-temperature cross polarization in view of enhancing dissolution dynamic nuclear polarization in NMR, *Chem. Phys. Lett.* 517 (4) (2011) 234–236.
- [14] S. Grzesiek, A. Bax, The importance of not saturating water in protein NMR. Application to sensitivity enhancement and NOE measurements, *J. Am. Chem. Soc.* 115 (26) (1993) 12593–12594.

- [15] J.-P. Demers, V. Vijayan, A. Lange, Recovery of bulk proton magnetization and sensitivity enhancement in ultrafast magic-angle spinning solid-state NMR, *J. Phys. Chem. B* 119 (7) (2015) 2908–2920.
- [16] R. Zhang, Y. Chen, N. Rodriguez-Hornedo, A. Ramamoorthy, Enhancing NMR sensitivity of natural-abundance low- $\gamma$  nuclei by ultrafast magic-angle-spinning solid-state NMR spectroscopy, *ChemPhysChem* 17 (19) (2016) 2962–2966.
- [17] D.A. Hall, D.C. Maus, G.J. Gerfen, S.J. Inati, L.R. Becerra, F.W. Dahlquist, R.G. Griffin, Polarization-enhanced NMR spectroscopy of biomolecules in frozen solution, *Science* 276 (5314) (1997) 930–932.
- [18] A. Lesage, M. Lelli, D. Gajan, M.A. Caporini, V. Vitzthum, P. Miéville, J. Alauzun, A. Roussey, C. Thieuleux, A. Mehdi, G. Bodenhausen, C. Coperet, L. Emsley, Surface enhanced NMR spectroscopy by dynamic nuclear polarization, *J. Am. Chem. Soc.* 132 (44) (2010) 15459–15461.
- [19] A.J. Rossini, A. Zagdoun, F. Hegner, M. Schwarzwälder, D. Gajan, C. Copéret, A. Lesage, L. Emsley, Dynamic nuclear polarization NMR spectroscopy of microcrystalline solids, *J. Am. Chem. Soc.* 134 (40) (2012) 16899–16908.
- [20] A.J. Rossini, C.M. Widdifield, A. Zagdoun, M. Lelli, M. Schwarzwälder, C. Copéret, A. Lesage, L. Emsley, Dynamic nuclear polarization enhanced nmr spectroscopy for pharmaceutical formulations, *J. Am. Chem. Soc.* 136 (6) (2014) 2324–2334.
- [21] L.R. Becerra, G.J. Gerfen, R.J. Temkin, D.J. Singel, R.G. Griffin, Dynamic nuclear-polarization with a cyclotron-resonance maser at 5-T, *Phys. Rev. Lett.* 71 (21) (1993) 3561–3564.
- [22] A.C. Pinon, J. Schlagnitweit, P. Berruyer, A.J. Rossini, M. Lelli, E. Socie, M. Tang, T. Pham, A. Lesage, S. Schantz, L. Emsley, Measuring nano- to microstructures from relayed dynamic nuclear polarization NMR, *J. Phys. Chem. C* 121 (29) (2017) 15993–16005.
- [23] A. Zagdoun, G. Casano, O. Ouari, M. Schwarzwälder, A.J. Rossini, F. Aussenac, M. Yulikov, G. Jeschke, C. Coperet, A. Lesage, P. Tordo, L. Emsley, Large molecular weight nitroxide biradicals providing efficient dynamic nuclear polarization at temperatures up to 200 K, *J. Am. Chem. Soc.* 135 (34) (2013) 12790–12797.
- [24] A. Zagdoun, A.J. Rossini, D. Gajan, A. Bourdolle, O. Ouari, M. Rosay, W.E. Maas, P. Tordo, M. Lelli, L. Emsley, A. Lesage, C. Copéret, Non-aqueous solvents for DNP surface enhanced NMR spectroscopy, *Chem. Commun.* 48 (5) (2011) 654–656.
- [25] M. Rosay, L. Tometich, S. Pawsey, R. Bader, R. Schauwecker, M. Blank, P.M. Borchard, S.R. Cauffman, K.L. Felch, R.T. Weber, R.J. Temkin, R.G. Griffin, W.E. Maas, Solid-state dynamic nuclear polarization at 263 GHz: spectrometer design and experimental results, *Phys. Chem. Chem. Phys.* 12 (22) (2010) 5850–5860.
- [26] D.J. Kubicki, A.J. Rossini, A. Porea, A. Zagdoun, O. Ouari, P. Tordo, F. Engelke, A. Lesage, L. Emsley, Amplifying dynamic nuclear polarization of frozen solutions by incorporating dielectric particles, *J. Am. Chem. Soc.* 136 (44) (2014) 15711–15718.
- [27] T.V. Can, M.A. Caporini, F. Mentink-Vigier, B. Corzilius, J.J. Walish, M. Rosay, W. E. Maas, M. Balduš, S. Vega, T.M. Swager, R.G. Griffin, Overhauser effects in insulating solids, *J. Chem. Phys.* 141 (6) (2014) 064202.
- [28] M. Lelli, S.R. Chaudhari, D. Gajan, G. Casano, A.J. Rossini, O. Ouari, P. Tordo, A. Lesage, L. Emsley, Solid-state dynamic nuclear polarization at 9.4 and 18.8 T from 100 K to room temperature, *J. Am. Chem. Soc.* 137 (46) (2015) 14558–14561.
- [29] A. Detken, E.H. Hardy, M. Ernst, B.H. Meier, Simple and efficient decoupling in magic-angle spinning solid-state NMR: the XiX scheme, *Chem. Phys. Lett.* 356 (3–4) (2002) 298–304.
- [30] K.R. Thurber, W.-M. Yau, R. Tycko, Low-temperature dynamic nuclear polarization at 9.4 T with a 30 mW microwave source, *J. Magn. Reson.* 204 (2) (2010) 303–313.
- [31] A.B. Barnes, G. De Paepe, P.C.A. van der Wel, K.N. Hu, C.G. Joo, V.S. Bajaj, M.L. Mak-Jurkauskas, J.R. Sirigiri, J. Herzfeld, R.J. Temkin, R.G. Griffin, High-field dynamic nuclear polarization for solid and solution biological NMR, *Appl. Magnet. Reson.* 34 (3–4) (2008) 237–263.
- [32] K.-N. Hu, G.T. Debelouchina, A.A. Smith, R.G. Griffin, Quantum mechanical theory of dynamic nuclear polarization in solid dielectrics, *J. Chem. Phys.* 134 (12) (2011) 125105.
- [33] A.J. Rossini, A. Zagdoun, M. Lelli, D. Gajan, F. Rascón, M. Rosay, W.E. Maas, C. Copéret, A. Lesage, L. Emsley, One hundred fold overall sensitivity enhancements for Silicon-29 NMR spectroscopy of surfaces by dynamic nuclear polarization with CPMG acquisition, *Chem. Sci.* 3 (1) (2012) 108–115.
- [34] G.T. Debelouchina, M.J. Bayro, P.C.A.v.d. Wel, M.A. Caporini, A.B. Barnes, M. Rosay, W.E. Maas, R.G. Griffin, Dynamic nuclear polarization-enhanced solid-state NMR spectroscopy of GNNQQNY nanocrystals and amyloid fibrils, *Phys. Chem. Chem. Phys.* 12 (22) (2010) 5911–5919.
- [35] J.R. Lewandowski, M.E. Halse, M. Blackledge, L. Emsley, Direct observation of hierarchical protein dynamics, *Science* 348 (6234) (2015) 578–581.
- [36] J.R. Yarava, S.R. Chaudhari, A.J. Rossini, A. Lesage, L. Emsley, Solvent suppression in DNP enhanced solid state NMR, *J. Magn. Reson.* 277 (Supplement C) (2017) 149–153.
- [37] A.C. Pinon, A.J. Rossini, C.M. Widdifield, D. Gajan, L. Emsley, Polymorphs of theophylline characterized by DNP enhanced solid-state NMR, *Mol. Pharmaceut.* 12 (11) (2015) 4146–4153.
- [38] A. Lesage, M. Bardet, L. Emsley, Through-bond carbon–carbon connectivities in disordered solids by NMR, *J. Am. Chem. Soc.* 121 (47) (1999) 10987–10993.